

RESEARCH ARTICLE

How fast is a collective bacterial state established?

Mikkel Lindstrøm Sørensen^{1,2}, Peter Dahl^{1,2}, Thomas Sams^{1*}

1 Biomedical Engineering, Dept. of Electrical Engineering, Technical University of Denmark, DK-2800 Lyngby, Denmark, **2** Dept. of Applied Mathematics and Computer Science, Technical University of Denmark, DK-2800 Lyngby, Denmark

☞ These authors contributed equally to this work.

* tsams@dtu.dk



Abstract

Bacteria in a biofilm colony have the capacity to monitor the size and growth conditions for the colony and modify their phenotypical behaviour to optimise attacks, defence, migration, etc. The quorum sensing systems controlling this involve production and sensing of diffusible signal molecules. Frequently, quorum sensing systems carry a positive feedback loop which produces a switch at a threshold size of the colony. This all-or-none switch can be beneficial to create a sudden attack, leaving a host little time to establish a defence. The reaction-diffusion system describing a basal quorum sensing loop involves production of signal molecules, diffusion of signal molecules, and detection of signal molecules. We study the ignition process in a numerical solution for a basal quorum sensor and demonstrate that even in a large colony the ignition travels through the whole colony in a less than a minute. The ignition of the positive feedback loop was examined in different approximations. As expected, in the exact calculation the ignition was found to be delayed compared to a calculation where the binding of signal molecules was quasistatic. The buffering of signal molecules is found to have little effect on the ignition process. Contrary to expectation, we find that the ignition does not start when the threshold is reached at the center—instead it allows for the threshold to be approached in the whole colony followed by an almost simultaneous ignition of the whole biofilm aggregate.

OPEN ACCESS

Citation: Sørensen ML, Dahl P, Sams T (2017) How fast is a collective bacterial state established? PLoS ONE 12(6): e0180199. <https://doi.org/10.1371/journal.pone.0180199>

Editor: Szabolcs Semsey, Niels Bohr Institute, DENMARK

Received: January 19, 2017

Accepted: June 12, 2017

Published: June 23, 2017

Copyright: © 2017 Sørensen et al. This is an open access article distributed under the terms of the [Creative Commons Attribution License](https://creativecommons.org/licenses/by/4.0/), which permits unrestricted use, distribution, and reproduction in any medium, provided the original author and source are credited.

Data Availability Statement: All relevant data are within the paper.

Funding: The authors received no specific funding for this work.

Competing interests: The authors have declared that no competing interests exist.

Introduction

Quorum sensing (QS) is a biological regulation process utilised by bacteria to control behaviour in accordance with size, density, and growth-rate of a bacterial population [1]. The process is based on diffusible signal molecules, produced by the bacteria at a background level. The signal molecules are able to bind to regulator molecules within the bacteria, thereby activating the regulator [2].

The collective behaviour regulated by QS was reported in *Vibrio fischeri* where it regulates camouflage light in large cell colonies in the host [3–5]. Since then, QS systems have been reported in many bacteria, e. g. *Aeromonas hydrophila* [6–9], *Agrobacterium tumefaciens* [10],

and *Pseudomonas aeruginosa* [11–13]. The presence of QS in colonies of bacteria appears to be the rule rather than the exception.

Frequently, the array of gene expressions acting under the control of activated QS regulators includes signal molecule synthetase. This positive feedback leads to a size-sensitive switch which can be used to control collective behaviour [1–5, 14]. The switch makes it possible to maintain an invisible state until the sudden QS regulated attack sets in. Recently, a proper measure of the “size” of a spherical biofilm aggregate was established as the cell density multiplied by the squared radius of the colony [15, 16]. The establishment of the size measure was based on the observation that the concentration of the activated regulator

$$r_a = [R_2S_2] \tag{1}$$

may be interpreted as the intrinsic measure of how quorate the state of the colony is and controls the quorum sensing feedback as well as QS regulated genes [15].

In small colonies the signal molecules are produced at a low background level. In larger colonies, the diffusive signal molecules accumulate, activate the transcriptional regulator, and induce transcription of the signal molecule synthetase at an increased level.

The dimer form of the activated regulator implied in Eq (1) allows for a fully developed switch in the ignition of the quorum as observed in Gram negative bacteria [3–5, 14]. The dimeric form is typical to quorum sensors and has been confirmed in main QS loops in a range of Gram negative bacteria [1, 12, 17–25]. In the present study we will study the time course of the ignition of the size-dependent switch in the most basic form of a single quorum sensitive switch.

Reaction-diffusion system

The quorum sensing system considered in this article, is based on the reaction-diffusion model proposed by Ferkinghoff-Borg and coworkers [15, 16, 25]. This model examines a dimer based regulator system with concentrations dependent on both spatial coordinates and time in a spherically symmetric geometry. These reaction-diffusion equations are obtained by considering the reactions that occur, when the unactivated regulator molecules dimerize and are subsequently activated by ligand binding as illustrated in Fig 1.

The reactions in Fig 1 are modelled by the four differential Eqs (2)–(5) [15].

$$\frac{\partial r_1}{\partial t} = b_1 + 2k_2^- r_2 - 2k_2^+ r_1^2 - \lambda_1 r_1 \tag{2}$$

$$\frac{\partial r_2}{\partial t} = k_2^+ r_1^2 + k_3^- r_3 - 2k_3^+ r_2 s - (k_2^- + \lambda_2) r_2 \tag{3}$$

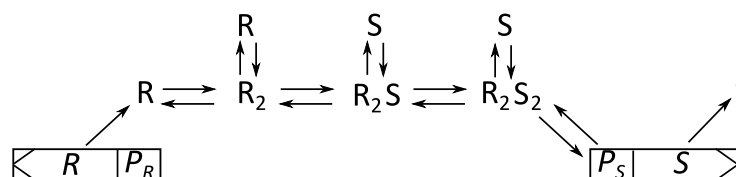


Fig 1. Reaction scheme of a generic quorum sensing process with regulator (R with promoter P_R) and signal molecules (S with promoter P_S). In this example dimerization takes place prior to signal molecule binding. As the signal molecules produced by the cell itself diffuse quickly away, the signal molecules binding to the regulator typically come from other cells. Figure modified from [15]

<https://doi.org/10.1371/journal.pone.0180199.g001>

$$\frac{\partial r_3}{\partial t} = 2k_3^+ r_2 s + 2k_4^- r_4 - k_4^+ r_3 s - (k_3^- + \lambda_3) r_3 \tag{4}$$

$$\frac{\partial r_4}{\partial t} = k_4^+ r_3 s - (2k_4^- + \lambda_4) r_4 \tag{5}$$

Each of the equations model the change in concentration of each regulator stage, with r_1 as the concentration of R, r_2 the concentration of R_2 and so forth. The final reaction produces the activated dimer regulator concentration $r_4 = r_a = [R_2 S_2]$.

The term b_1 signifies the production of monomer regulator with concentration $r_1 = [R]$. In the model the reaction between regulators is governed by on- and off-rates, denoted by k_i^+ and k_i^- , as well as degradation rates λ_i , $i = 1, \dots, 4$. The dimer degradation rates are assumed to be equal $\lambda_d = \lambda_2 = \lambda_3 = \lambda_4$ [16] and significantly lower than the monomer decay rate λ_1 . All degradation rates include proteolytic degradation as well as dilution by cell division. The degradation rates are assumed to be considerably slower than the on- and off-rates.

Additionally, an equation governing the production and diffusion of signal molecules is required. The change in signal molecule concentration $s = [S]$ is modelled using a diffusion equation containing a production term $\rho_v \kappa_s$:

$$\frac{\partial s}{\partial t} = D\Delta s + \rho_v \kappa_s \tag{6}$$

$$\kappa_s = \frac{\frac{b_s}{k_s} K_s + r_a}{K_s + r_a} k_s \approx \begin{cases} b_s & , r_a < \frac{b_s}{k_s} K_s \\ k_s & , r_a > K_s \end{cases} \tag{7}$$

Multiplication of the intracellular production κ_s by the volume fraction occupied by cells, ρ_v , ensures correct normalisation of the production term. Note that the production term shifts away from background production, $\rho_v b_s$, already when the activated regulator level reaches $\frac{b_s}{k_s} K_s$, which was recognised as the ignition point for the feed-back loop [15].

When solving the model numerically, a spherical geometry with radius \mathcal{R} will be assumed. Regulator as well as signal molecule concentrations are thus dependent on time, t , and distance from center. Additionally, the boundary of the colony is assumed to be absorbing, $s(\mathcal{R}, t) = 0$, corresponding to a rapid exchange of the surroundings.

Eq (6) implicitly assumes that the free signal molecule concentration is much larger than the bound signal molecule concentration. If this is not the case, for a calculation of the time course of the binding, it is necessary to account for the bound signal molecules. This results in the following equation.

$$\frac{\partial s}{\partial t} = D\Delta s + \rho_v \kappa_s + \rho_v (2k_4^- r_4 + k_3^- r_3 - 2k_3^+ r_2 s - k_4^+ r_3 s) \tag{8}$$

Incorporating this behaviour in the model, introduces a buffering of the signal molecules. In the static limit, the added terms vanish and therefore do not alter the results by Ferkinghoff-Borg *et al.* Below, we shall refer to the solution of Eqs (2)–(5) with Eq (8) as the “exact” model, and the solution with Eq (6) as the solution “without buffering”.

In Eq (6) we only consider the generic case, where there is equilibrium between the concentration of signal molecules inside and outside the cells. This is a fair approximation for QS systems mediated by smaller AHL molecules. However, for larger AHL molecules, active efflux

pumps have been reported to assist in transporting the autoinducers out of the cell thereby speeding up the ignition process [26, 27]. Modifications representing the active transport across the membrane may therefore have to be introduced to produce a realistic profile of the ignition process in these cases [28].

Quasi-static and static approximations to the solution of the reaction-diffusion system will serve as references for the obtained results. The quasi-static approximation assumes an instant equilibrium between regulator stages Eqs (2)–(5). This leads to a simple relation between signal molecule concentration and activated regulator concentration

$$r_4 = r_a = \frac{s^2}{\tilde{K}^2 + s^2} r_m \tag{9}$$

where r_m is the maximal concentration of the active form of the regulator and \tilde{K} is an effective dissociation constant which sits at the crossing between the asymptotes for large and small signal molecule concentrations [29]. Both r_m and \tilde{K} are determined by the static solution of Eqs (2)–(5). The quasi-static approximation does not assume the diffusion equation to be in static equilibrium.

The static approximation of the model leads to an instantaneous switch and can be solved by letting all time derivatives vanish [15]. At the center of the colony, the static approximation

Table 1. Table of parameters.

Parameter	Value	Description	Reference
b_1	1000 nM/h	Monomer regulator production rate	[32, 33]
D	~ 2 mm ² /h	Diffusion constant	[15, 34]
b_s	3600 nM/h	Background production of S	[33]
k_s	100 b_s	Maximum production of S	[15]
K_s	1 nM	Promoter site P_S dissociation constant	Current study
r_1		R concentration	
r_2		R_2 concentration	
r_3		R_2S concentration	
$r_4 = r_a$	< r_m	R_2S_2 activated regulator concentration	
r_m	537 nM	Maximal r_a concentration	
\tilde{K}	208 nM	Effective dissociation constant	[9, 35–37]
\mathcal{R}	100 μ m	Radius of colony	[38–41]
ρ_v		Cell density (volume fraction occupied by cells)	
k_2^-	1000 h ⁻¹	$2R \leftarrow R_2$ rate	[33]
k_2^+	0.5 nM ⁻¹ h ⁻¹	$2R \rightarrow R_2$ rate constant	[33, 42, 43]
k_3^-	1000 h ⁻¹	$R_2 + S \leftarrow R_2S$ rate	[33]
k_3^+	100 nM ⁻¹ h ⁻¹	$R_2 + S \rightarrow R_2S$ rate constant	[33]
k_4^-	1000 h ⁻¹	$R_2S + S \leftarrow R_2S_2$ rate	[33]
k_4^+	100 nM ⁻¹ h ⁻¹	$R_2S + S \rightarrow R_2S_2$ rate constant	[33]
λ_1	20 h ⁻¹	Monomer decay rate	[17, 18]
λ_d	0.5 h ⁻¹	Dimer decay rate ($\lambda_2, \lambda_3, \lambda_4$)	[1, 24, 25]
λ_0	0.5 h ⁻¹	cell density growth rate	

Table containing descriptions and values of parameters used in the model.

<https://doi.org/10.1371/journal.pone.0180199.t001>

yields a simple factorised expression for the size of a colony, Σ ,

$$\Sigma = \frac{1}{3} \mathcal{R}^2 \rho_v = \frac{2D\tilde{K}}{b_s} \underbrace{\frac{b_s K_s + r_a}{k_s \frac{b_s}{k_s} K_s + r_a}}_{\text{feedback switch}} \underbrace{\left(\frac{r_a}{r_m - r_a} \right)^{1/2}}_{\text{forward switch}} \quad (10)$$

dependent on the activated regulator concentration, r_a , [15]. Here all geometrical properties (density and radius of the colony) are conveniently on the lhs. of the equation, and all intracellular properties are on the rhs. The braces enhance the role of each term in the factorised form. This factorized expression assumes not only time independence but also constant activation

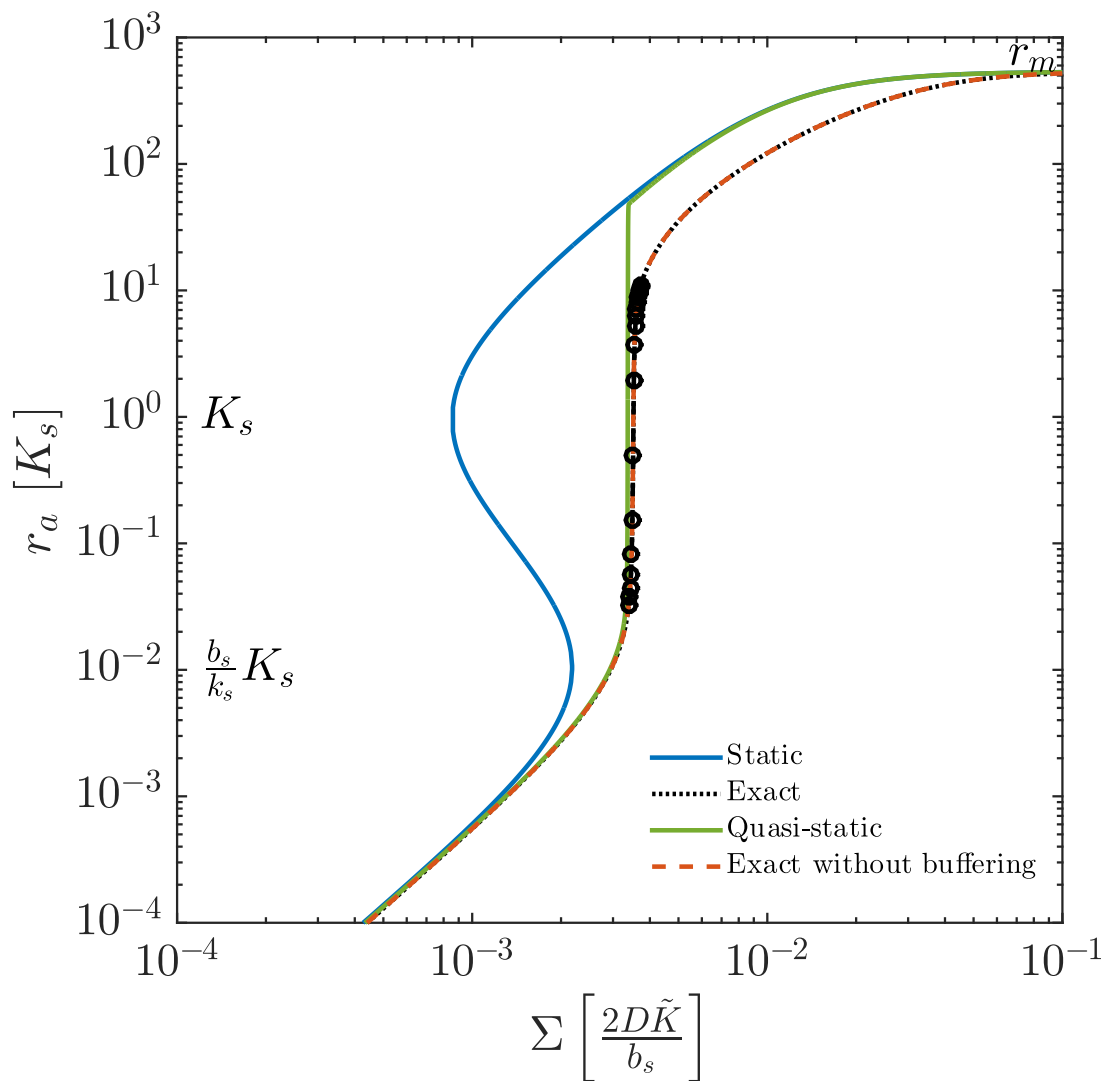


Fig 2. Plot of activated regulator concentration, $r_a = r_a$, at the center of the colony as a function of geometric size measure, Σ . Both axes are in natural units. The exact solution depicts the solution found when solving Eqs (2)–(5) and (8), whereas non-buffered solution uses Eq (6). The quasi-static solution uses Eqs (6) and (9). The ignition point, $r_a = \frac{b_s}{k_s} K_s = 10^{-2} K_s$, is indicated, as well as the dissociation constant K_s and maximum regulator concentration r_m . The exact solution is displayed with circles corresponding to 10 second intervals to indicate the speed of the ignition.

<https://doi.org/10.1371/journal.pone.0180199.g002>

throughout the micro colony. Nevertheless, it proves to describe the qualitative features of the system.

The system of differential equations was solved using the numerical solver *pdepe* in Matlab [30, 31]. The initial condition was established by keeping the cell density fixed at a value below the ignition point and allowing the system develop to stationary state. Growth of the colony size, Σ , was accomplished by increasing the cell density, ρ_v , at a rate $\lambda_0 = 0.5 \text{ h}^{-1}$. The full set of parameters used in the simulation is listed in Table 1.

Results and analysis

In Fig 2, the activated regulator concentration at the center of the colony, r_a , is displayed as a function of the size, Σ . The curves represent the full model with and without buffering (broken lines) compared with the static and quasi-static solutions (full lines).

First, we note that the exact model with buffering is indistinguishable from the model without buffering, thus indicating that buffering of the signal molecules does not play a significant role.

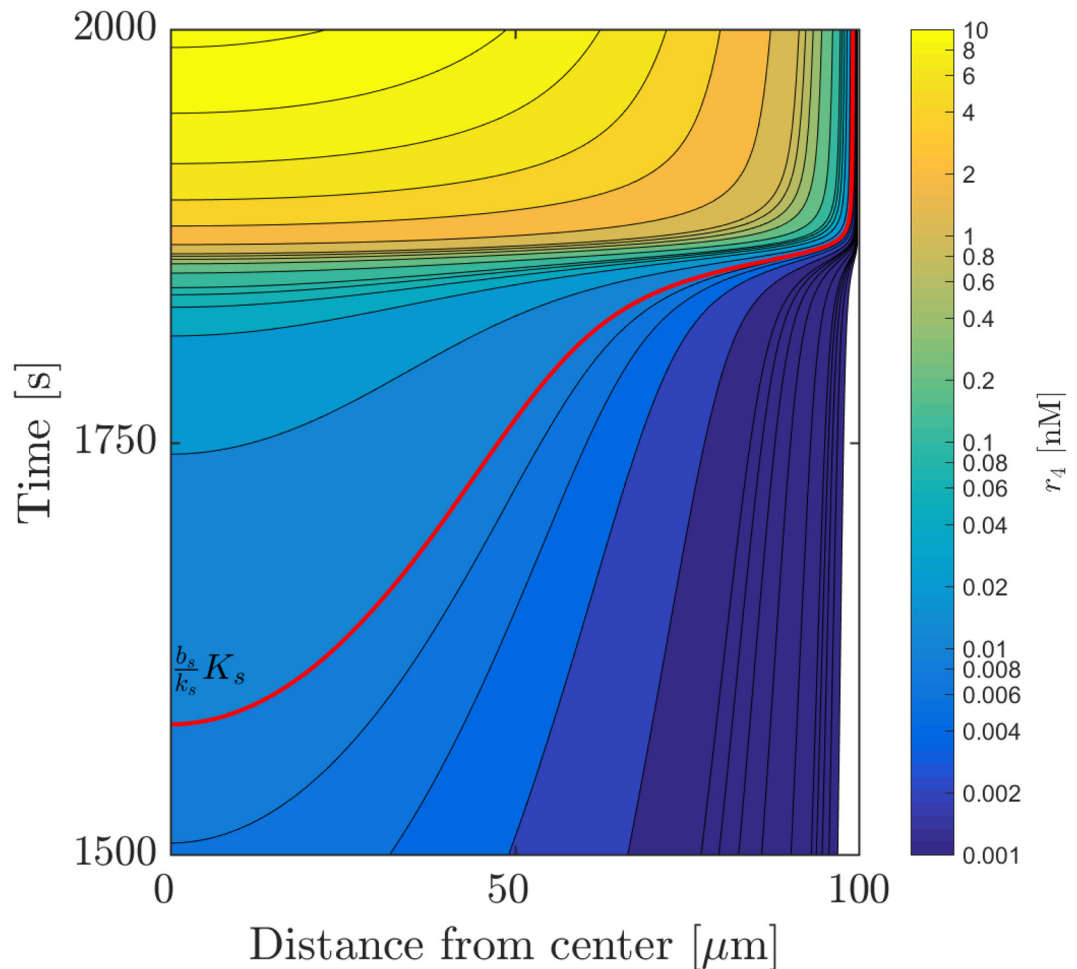


Fig 3. Contour plot of activated regulator concentration $r_a = r_4 = [R_2S_2]$ around the time of ignition as a function of time and distance from the center of the colony. The plot contains the exact solution of the system of equations presented in Eqs (2)–(5) as well as Eq (8), i. e. the system describing total signal molecule concentration. The concentration necessary for ignition ($\frac{b_s}{k_s} K_s$ in the static case) is marked by the red contour. A logarithmic colour-scheme has been chosen due to the large range of values pre- and post-ignition.

<https://doi.org/10.1371/journal.pone.0180199.g003>

In the factorized static approximation by Ferkinghoff-Borg *et al.* the feed-back loop appears to ignite at a somewhat lower size than the full solution and the quasi-static solutions. This is due to the approximation, that the concentration of activated regulator is taken to be equal to its value at the center throughout the colony. It therefore reflects a limitation of the simple factorized model in Eq (10).

The quasi-static solution resembles the exact solution, differing only slightly around the time of ignition. As expected, the ignition of the system occurs prior to the ignition in the exact solution. In contrast to the quasi-static solution, at ignition, the full solution jumps only part of the way up to the factorized static solution. The reason for this difference is that, in the full model, the dimer concentration needs to build up and does so at the same rate as the dilution from growth and degradation in the cells. The exact and quasi-static solutions show an increase of more than two decades in activated regulator concentration, shortly after reaching the ignition point. Examining the circles, it can be seen that the ignition takes less than a minute. (Here we define “ignition” as a jump of 2 orders of magnitude in concentration of activated regulator, r_a .)

The activation of the feed-back loop as a function of the radial coordinate and time may be examined in Fig 3. The ignition concentration ($\sim \frac{b}{k_s} K_s$) is reached at different times throughout the colony, with a difference of approximately 5 minutes between the ignition point at the center and the ignition point close to the boundary. However, the ignition, recognized as dense horizontal lines, does not occur until the ignition condition is reached throughout the whole colony. Once this happens, the whole colony ignites in less than a minute, ignoring a thin region near the boundary which is under the control of the boundary condition. Thus, the contour plot confirms the expectation that the entire colony resides in a well defined state, either on or off.

Conclusion

We have modelled a generic single-loop quorum sensing system with positive feedback. The primary goal of the study has been to study of the space-time structure of the ignition of the switch produced by the positive feedback in the quorum sensor.

The exact solution exhibits a delayed response compared to both the quasi-static and static approximations, as it is limited by the time it takes the regulator stages to react and build up concentration of activated regulator. Inclusion of buffering terms produces no further retardation of the system.

Using a 3D representation to depict both the spatial and temporal dependency of the activated regulator concentration, the collective behaviour of the colony could be studied. A slow build-up over five minutes to the ignition concentration of activated regulator followed by a quick ignition was observed. The process exhibits the desired behaviour, as the entire colony is either in an on- or off-state. These observations indicate that a partial ignition is difficult to achieve, even for slow systems. The model demonstrates that even the largest naturally occurring biofilm aggregates in chronic infections [41] ignite fully in less than a minute and, truly, can be said to produce a surprise attack.

Author Contributions

Conceptualization: MLS PD TS.

Formal analysis: MLS PD TS.

Methodology: MLS PD TS.

Software: MLS PD.

Supervision: TS.

Visualization: MLS PD TS.

Writing – original draft: MLS PD TS.

Writing – review & editing: MLS PD TS.

References

1. Gonzalez JE, Keshavan ND. Messing with Bacterial Quorum Sensing. *Microbiology & Molecular Biology Reviews*. 2006; 70(4):1.
2. Smith KM, Bu Y, Suga H. Induction and Inhibition of *Pseudomonas aeruginosa* Quorum Sensing by Synthetic Autoinducer Analogs. *Chemistry & Biology*. 2003; 10(1):81–89. [https://doi.org/10.1016/S1074-5521\(03\)00002-4](https://doi.org/10.1016/S1074-5521(03)00002-4)
3. Neelson KH, Platt T, Hastings JW. Cellular control of the synthesis and activity of the bacterial luminescence system. *J Bacteriol*. 1970; 104:313–322. PMID: [5473898](https://pubmed.ncbi.nlm.nih.gov/5473898/)
4. Eberhard A. Inhibition and activation of bacterial luciferase synthesis. *J Bacteriology*. 1972; 109:1101.
5. Choi SH, Greenberg EP. Genetic dissection of DNA binding and luminescence gene activation by the *Vibrio fischeri* LuxR protein. *J Bacteriology*. 1992; 174:4064–69. <https://doi.org/10.1128/jb.174.12.4064-4069.1992>
6. Swift S, Karlyshev AV, Durant EL, Winson MK, Chhabra SR, Williams P, et al. Quorum sensing in *Aeromonas hydrophila* and *Aeromonas salmonicida*: identification of the LuxRI homologues AhyRI and AsaRI and their cognate signal molecules. *Journal of Bacteriology*. 1997; 179:5271–5282. <https://doi.org/10.1128/jb.179.17.5271-5281.1997> PMID: [9286976](https://pubmed.ncbi.nlm.nih.gov/9286976/)
7. Lynch MJ, Swift S, Kirke DF, Keevil CW, Dodd CER, Williams P. The regulation of biofilm development by quorum sensing in *Aeromonas hydrophila*. *Environmental Microbiology*. 2002; 4:18–28. <https://doi.org/10.1046/j.1462-2920.2002.00264.x> PMID: [11966822](https://pubmed.ncbi.nlm.nih.gov/11966822/)
8. Kirke DF, Swift S, Lynch MJ, Williams P. The *Aeromonas hydrophila* LuxR homologue AhyR regulates the *N*-acyl homoserine lactone synthase, Ahyl positively and negatively in a growth phase-dependent manner. *FEMS Microbiology Letters*. 2004; 241:109–117. <https://doi.org/10.1016/j.femsle.2004.10.011> PMID: [15556717](https://pubmed.ncbi.nlm.nih.gov/15556717/)
9. Garde C, Bjarnsholt T, Givskov M, Jakobsen TH, Hentzer M, Claussen A, et al. Quorum Sensing regulation in *Aeromonas hydrophila*. *Journal of Molecular Biology*. 2010; 396:849–857. <https://doi.org/10.1016/j.jmb.2010.01.002> PMID: [20064524](https://pubmed.ncbi.nlm.nih.gov/20064524/)
10. Bottomley MJ, Muraglia E, Bazzo R, Carfi A. Molecular insights into quorum sensing in the human pathogen *Pseudomonas aeruginosa* from the structure of the virulence regulator LasR bound to its autoinducer. *Journal of Biological Chemistry*. 2007; 282(18):13592–13600. <https://doi.org/10.1074/jbc.M700556200> PMID: [17363368](https://pubmed.ncbi.nlm.nih.gov/17363368/)
11. Fuqua WC, Winans SC, Greenberg EP. Quorum sensing in bacteria: The LuxR-LuxI family of cell density-responsive transcriptional regulators. *Journal of Bacteriology*. 1994; 176(2):269–275. <https://doi.org/10.1128/jb.176.2.269-275.1994> PMID: [8288518](https://pubmed.ncbi.nlm.nih.gov/8288518/)
12. Fuqua C, Winans SC, Greenberg EP. Census and Consensus in Bacterial Ecosystems: The LuxR-LuxI Family of Quorum-Sensing Transcriptional Regulators. *Annual Review of Microbiology*. 1996; 50:727–753. <https://doi.org/10.1146/annurev.micro.50.1.727> PMID: [8905097](https://pubmed.ncbi.nlm.nih.gov/8905097/)
13. Moré MI, Finger LD, Stryker JL, Fuqua C, Eberhard A, Winans SC. Enzymatic Synthesis of a Quorum-Sensing Autoinducer Through Use of Defined Substrates. *Science*. 1996; 272(5268):1655–1658. <https://doi.org/10.1126/science.272.5268.1655> PMID: [8658141](https://pubmed.ncbi.nlm.nih.gov/8658141/)
14. Hanzelka BL, Greenberg EP. Evidence that the N-terminal region of the *Vibrio fischeri* LuxR protein constitutes an autoinducer-binding domain. *J Bacteriology*. 1995; 177(3):815–17. <https://doi.org/10.1128/jb.177.3.815-817.1995>
15. Ferkinghoff-Borg J, Sams T. Size of quorum sensing communities. *Mol BioSyst*. 2014; 10:103–109. <https://doi.org/10.1039/C3MB70230H> PMID: [24162891](https://pubmed.ncbi.nlm.nih.gov/24162891/)
16. Garde C, Welch M, Ferkinghoff-Borg J, Sams T. Microbial Biofilm as a Smart Material. *Sensors*. 2015; 15(2):4229–4241. <https://doi.org/10.3390/s150204229> PMID: [25686310](https://pubmed.ncbi.nlm.nih.gov/25686310/)
17. Zhu J, Winans SC. Autoinducer binding by the quorum-sensing regulator TraR increases affinity for target promoters *in vitro* and decreases TraR turnover rates in whole cells. *Proc Natl Acad Sci USA*. 1999; 96:4832–37. <https://doi.org/10.1073/pnas.96.9.4832> PMID: [10220379](https://pubmed.ncbi.nlm.nih.gov/10220379/)

18. Zhu J, Winans SC. The quorum-sensing transcriptional regulator TraR requires its cognate signaling ligand for protein folding, protease resistance, and dimerization. *Proc Natl Acad Sci USA*. 2001; 98:1507–12. <https://doi.org/10.1073/pnas.98.4.1507> PMID: 11171981
19. Ventre I, Ledgham F, Prima V, Lazdunski A, Foglino M, Sturgis JN. Dimerization of the quorum sensing regulator RhlR: development of a method using EGFP fluorescence anisotropy. *Molecular Microbiology*. 2003; 48:187–198. <https://doi.org/10.1046/j.1365-2958.2003.03422.x> PMID: 12657054
20. Schuster M, Lostroh CP, Ogi T, Greenberg EP. Identification, timing, and signal specificity of *Pseudomonas aeruginosa* quorum-controlled genes: A transcriptome analysis. *Journal of Bacteriology*. 2003; 185(7):2066–2079. <https://doi.org/10.1128/JB.185.7.2066-2079.2003> PMID: 12644476
21. Schuster M, Urbanowski ML, Greenberg EP. Promoter Specificity in *Pseudomonas aeruginosa* Quorum Sensing Revealed by DNA Binding of Purified LasR. *Proceedings of the National Academy of Sciences of the United States of America*. 2004; 101(45):15833–15839 and 3373727. <https://doi.org/10.1073/pnas.0407229101> PMID: 15505212
22. Abeliovich H. An Empirical Extremum Principle for the Hill Coefficient in Ligand-Protein Interactions Showing Negative Cooperativity. *Biophysical Journal*. 2005; 89(1):76–79. <http://dx.doi.org/10.1529/biophysj.105.060194>. PMID: 15834004
23. Pinto UM, Winans SC. Dimerization of the quorum-sensing transcription factor TraR enhances resistance to cytoplasmic proteolysis. *Molecular Microbiology*. 2009; 73(1):32–42. <https://doi.org/10.1111/j.1365-2958.2009.06730.x> PMID: 19432796
24. Sappington KJ, Dandekar AA, Oinuma KI, Greenberg EP. Reversible Signal Binding by the *Pseudomonas aeruginosa* Quorum-Sensing Signal Receptor LasR. *mBio*. 2011; 2(1):e00011–11. <https://doi.org/10.1128/mBio.00011-11> PMID: 21325039
25. Claussen A, Jakobsen TH, Bjarnsholt T, Givskov M, Welch M, Ferkinghoff-Borg J, et al. Kinetic Model for Signal Binding to the Quorum Sensing Regulator LasR. *International Journal of Molecular Sciences*. 2013; 14(7):13360–13376. <https://doi.org/10.3390/ijms140713360> PMID: 23807499
26. Boyer M, Wisniewski-Dyé F. Cell–cell signalling in bacteria: not simply a matter of quorum. *FEMS Microbiology Ecology*. 2009; 70(1):1–19. <https://doi.org/10.1111/j.1574-6941.2009.00745.x> PMID: 19689448
27. Pearson JP, van Delden C, Iglewski BH. Active efflux and diffusion are involved in transport of *Pseudomonas aeruginosa* cell-to-cell signals. *Journal of Bacteriology*. 1999; 181(4):1203–1210. PMID: 9973347
28. Pai A, You L. Optimal tuning of bacterial sensing potential. *Molecular Systems Biology*. 2009; 5:286. <https://doi.org/10.1038/msb.2009.43> PMID: 19584835
29. Sams T. Effective dissociation constants and cooperativity in activation of transcription factors. Manuscript in preparation, 2017.
30. Skeel R, Berzins M. A Method for the Spatial Discretization of Parabolic Equations in one Space Variable. *SIAM Journal on Scientific and Statistical Computing*. 1990; 11(1):1–32. <https://doi.org/10.1137/0911001>
31. The Mathworks I. MATLAB version 9.1.0.441655 (R2016b); 2016.
32. Fagerlind M, Rice S, Nilsson P, Harlen M, James S, Charlton T, et al. The role of regulators in the expression of quorum-sensing signals in *Pseudomonas aeruginosa*. *Journal of Molecular Microbiology and Biotechnology*. 2003; 6(2):88–100. <https://doi.org/10.1159/000076739> PMID: 15044827
33. Fagerlind MG, Nilsson P, Harlén M, Karlsson S, Rice SA, Kjelleberg S. Modeling the effect of acylated homoserine lactone antagonists in *Pseudomonas aeruginosa*. *BioSystems*. 2005; 80:201–213. <https://doi.org/10.1016/j.biosystems.2004.11.008> PMID: 15823419
34. Trovato A, Seno F, Zanardo M, Alberghini S, Tondello A, Squartini A. Quorum vs. diffusion sensing: A quantitative analysis of the relevance of absorbing or reflecting boundaries. *Fems Microbiology Letters*. 2014; 352(2):198–203. <https://doi.org/10.1111/1574-6968.12394> PMID: 24484313
35. Andersen JB, Sternberg C, Poulsen LK, Bjorn SP, Givskov M, Molin S. New Unstable Variants of Green Fluorescent Protein for Studies of Transient Gene Expression in Bacteria. *Applied and Environmental Microbiology*. 1998; 64:2240–46. PMID: 9603842
36. Welch M, Todd DE, Whitehead NA, McGowan SJ, Bycroft BW, Salmond GP. *N*-acyl homoserine lactone binding to the CarR receptor determines quorum-sensing specificity in *Erwinia*. *The EMBO journal*. 2000; 19(4):631–641. <https://doi.org/10.1093/emboj/19.4.631> PMID: 10675332
37. Welch M, Gross J, Hodgkinson JT, Spring DR, Sams T. Ligand binding kinetics of the quorum sensing regulator PqsR. *Biochemistry*. 2013; 52(25):4433–4438. <https://doi.org/10.1021/bi400315s> PMID: 23713667

38. Stewart PS, Peyton BM, Drury WJ, Murga R. Quantitative observations of heterogeneities in *Pseudomonas aeruginosa* biofilms. *Applied and Environmental Microbiology*. 1993; 59(1):327–329. PMID: [8439159](#)
39. Stoodley P, Lewandowski Z, Boyle JD, Lappin-Scott HM. Structural deformation of bacterial biofilms caused by short-term fluctuations in fluid shear: An in situ investigation of biofilm rheology. *Biotechnology and Bioengineering*. 1999; 65(1):83–92. PMID: [10440674](#)
40. Jefferson KK, Goldmann DA, Pier GB. Use of confocal microscopy to analyze the rate of vancomycin penetration through *Staphylococcus aureus* biofilms. *Antimicrobial Agents and Chemotherapy*. 2005; 49(6):2467–2473. <https://doi.org/10.1128/AAC.49.6.2467-2473.2005> PMID: [15917548](#)
41. Bjarnsholt T, Alhede M, Alhede M, Eickhardt-Sørensen S, Moser C, Kühl M, et al. The in vivo biofilm. *Trends in Microbiology*. 2013; 21(9):466–474. <https://doi.org/10.1016/j.tim.2013.06.002> PMID: [23827084](#)
42. Schlosshauer M, Baker D. Realistic protein-protein association rates from a simple diffusional model neglecting long-range interactions, free energy barriers, and landscape ruggedness. *Protein Sci*. 2004; 13(6):1660–1669. <https://doi.org/10.1110/ps.03517304> PMID: [15133165](#)
43. Schlosshauer M, Baker D. A General Expression for Bimolecular Association Rates with Orientational Constraints. *J Phys Chem B*. 2002; 106:12079–12083. <https://doi.org/10.1021/jp025894j>